Available online at www.sciencedirect.com

SciVerse ScienceDirect

journal homepage: www.elsevier.com/locate/watres

Pyrosequencing reveals higher impact of silver nanoparticles than Ag^+ on the microbial community structure of activated sludge

Yu Yang [a], John Quensen [b,c], Jacques Mathieu [a], Qiong Wang [b], Jing Wang [a], Mengyan Li [a], James M. Tiedje [b,c], Pedro J.J. Alvarez [a,*]

[a] Department of Civil & Environmental Engineering, Rice University, Houston, TX 77005, USA
[b] Center for Microbial Ecology, Michigan State University, East Lansing, MI 48823, USA
[c] Department of Crop & Soil Science, Michigan State University, East Lansing, MI 48823, USA

ARTICLE INFO

Article history:
Received 25 July 2013
Received in revised form
20 September 2013
Accepted 22 September 2013
Available online 5 October 2013

Keywords:
Activated sludge
Silver nanoparticles
Floc
Pyrosequencing
Nitrification

ABSTRACT

Although the antimicrobial capabilities of silver nanoparticles (AgNPs) are widely reported, their impacts on ecologically important microbial communities are not well understood. AgNPs released from consumer products will likely enter sewer systems and wastewater treatment plants, where they would encounter (and potentially upset) activated sludge (AS), a complex ecosystem containing a variety of bacteria. Herein we address the effects of AgNPs and Ag^+ ions on the microbial community structure of AS, using pyrosequencing technology. Compared to Ag^+ amendment, a lower AgNP concentration resulted in a more pronounced effect on AS community structure, possibly reflecting a higher propensity of Ag^+ than AgNPs to be scavenged by inorganic ligands and organic matter. Furthermore, AgNPs decreased the abundance of nitrifying bacteria, which would hinder N removal, and damaged AS floc structure, which could affect sludge clarification and recycling. Overall, although released Ag^+ is known to be the critical effector of the antimicrobial activity of AgNPs, the nanoparticles apparently delivered Ag^+ to bacteria more effectively and exerted more pronounced microbial population shifts that would hinder some wastewater treatment processes.

Published by Elsevier Ltd.

1. Introduction

More than 1300 nanotechnology-enabled products have already entered the market (The Project on Emerging Nanotechnologies). This rapid increase (greater than 500% over the past five years) is of concern because the long-term consequences of chronic exposure to nanoparticles are still unknown. By far, the most commonly utilized commercial nanomaterials are antimicrobial silver nanoparticles (AgNPs), which can be found in personal care products, laundry additives, clothes and paintings (Ip et al. 2006; Klasen, 2000; Simpson, 2003).

Material flow analysis suggests that the majority of AgNPs released from consumer products enter sewer systems and wastewater treatment plants (WWTPs) (Gottschalk et al. 2009; Kaegi et al. 2011). Activated sludge (AS) microbial communities are already being exposed to various forms of silver, and a range of 1.8–105 ppb in sewage reaching WWTPs

* *Corresponding author*. Tel.: +1 713 348 5903; fax: +1 713 348 5203.
E-mail address: alvarez@rice.edu (P.J.J. Alvarez).

0043-1354/$ – see front matter Published by Elsevier Ltd.
http://dx.doi.org/10.1016/j.watres.2013.09.046

(Shafer et al. 1998) and 2–195 ppm in discarded biosolids (Radniecki et al. 2011) were reported, indicating that AS is a likely sink for AgNPs. One dominant type of silver particles found in AS plants is nano-sized Ag_2S (Kim et al. 2010), which are formed when AgNPs or Ag^+ ions react with sulfides produced in sewage collection systems or other anaerobic environments. Larger AgNPs often maintain a core Ag shell with a passivating Ag_2S surface layer (Kaegi et al. 2011). AgNPs also commonly harbor Ag_2O, which is known to release antimicrobial silver ions (Ag^+) (Liu et al. 2010).

Depending on the concentrations present, silver could upset the operation of AS plants, and inhibition of biological nitrogen removal (specifically nitrification) by AgNPs (1–20 ppm) has been previously reported (Arnaout and Gunsch, 2012; Choi and Hu, 2009; Liang et al. 2010). However, it is unknown how sub-lethal concentrations of AgNPs and the silver ions (Ag^+) that they release affect the structure of the AS microbial community and the resulting functional diversity.

Pyrosequencing is a high-throughput DNA sequencing method that enables quantitative characterization of complex microbial communities, such as those in soil (Ge et al. 2012), seawater (Qian et al. 2011), human intestines (Claesson et al. 2009), and WWTPs (Zhang et al. 2012). Here, we used pyrosequencing to investigate how AS exposure to AgNPs or Ag^+ affects microbial community structure, which has important implications for AS process performance. We compared the effects of AgNPs and Ag^+, quantified the change in abundance of specific microbial species in response to different forms of silver, and identified species that were particularly sensitive or resistant to AgNPs. Additionally, we investigated the impact of AgNPs on AS floc structure.

2. Materials and methods

2.1. AS microcosm test

AS samples were collected from the 69th Street WWTP (Houston, TX), which normally operates with a mixed liquor suspended solids concentration of about 2000 mg/L. Chemical and physical properties of the AS sample (e.g., dissolved organic matter, pH, NO_3^-, NH_4^+, Cl^-, SO_4^{2-} and PO_4^{3-} concentrations) were characterized by ALS Laboratory group (Houston, TX). After the AS samples were collected, they were immediately exposed to different forms of silver added at different concentrations to account for differences in their antimicrobial activity. AS samples (10 mL) were exposed to 5-nm AgNPs (0.05 ppm), 35-nm AgNPs (40 ppm) or Ag^+ (1 ppm, added as $AgNO_3$) at 26 °C for 7 days. These silver concentrations fall within a representative range (Radniecki et al. 2011; Shafer et al. 1998), and were selected based on preliminary toxicity assessments to exert similar effects: these concentrations exerted a similar inhibition on AS oxygen consumption (24–28% reduction) (Table S1), as determined with a PF-8000 respirometer (RSA, Inc., Springdale, AR). The exposed samples and control were prepared in triplicate. Ammonia concentrations were measured at days 0, 1, 3, 5 and 7 with an ICS-1600 standard integrated IC system (Dionex, Sunnyvale, CA) using 20 mM methanesulfonic acid as the eluent. Phosphate and nitrate were monitored with a DX600 ion chromatograph (Dionex, Sunnyvale, CA) equipped with an ED50 electrochemical detector and a RFIC™ IonPac® S11-HC column with NaOH (30 mM) as the mobile phase (Yang et al. 2011). For the Ag^+ released from AgNPs, the supernatant was collected after 1 ml of the sample in each microcosm was ultracentrifuged (35,000 rpm for 4 h) (Yang et al. 2012). The supernatant was then treated with HNO_3 (final concentration around 1%). All the silver concentrations were measured by Inductively-coupled plasma mass spectrometry (ICP-MS) using an Elan 9000 instrument (Perkin–Elmer, Waltham, MA).

2.2. Pyrosequencing

Two milliliter samples from each microcosm were centrifuged at 5000 r.p.m. for 10 min at 4 °C, and the pellets were collected for DNA extraction with a soil extraction kit (Mobio, Inc., San Diego, CA). rRNA genes were amplified for pyrosequencing using a primer set that captured the V4 hypervariable region of the 16S rRNA genes into the beginning of V6 at corresponding *Escherichia coli* positions 577 and 926: primers 577F (5′-**CGTATCGCCTCCCTCGCGCCATCAG**[bar code]AYTGGGYDTAAAGNG-3′) and 926R (5′-**CTATGCGCCTTGCCAGCCCGCTCAG**CCGTCAATTCMTTTRAGT-3′), where the sequencing adaptors are in boldface. The forward primers contained a short run of nucleotides used as bar codes that were distinct from each other by at least two nucleotides. The PCR mixture contained 1 μM each primer, 1.8 mM $MgCl_2$, 0.2 mM each deoxynucleoside triphosphate, 3 μg bovine serum albumin, 1 U of the FastStart high-fidelity PCR system enzyme blend and 10 ng of DNA template. Amplification was conducted using the following PCR conditions: 95 °C for 3 min; 30 cycles of 95 °C for 45 s, 57 °C for 30 s and 72 °C for 1 min; and 72 °C for 4 min. PCR products were separated on a 1% agarose Tris-acetate-EDTA gel, and bands between 400 and 450 bp were excised. The bands were extracted with a QIAquick gel extraction kit (Qiagen Inc. Valencia, CA), purified with a QIAquick PCR purification kit, and eluted in 20 μl of EB buffer (10 mMTris-Cl, pH 8.5). Clean products were quantified with an ND-1000 spectrophotometer (Nanodrop Technologies, Wilmington, DE) and mixed in equal amounts (20 ng each) for sequencing by a Genome Sequencer FLX system (454; Life Sciences).

2.3. Sequence processing

All the raw reads were processed with Ribosomal Database Project (RDP) Pyrosequencing Pipeline (http://pyro.cme.msu.edu) (Cole et al. 2009). Sequences were first trimmed to remove the adaptor sequences and then sorted based on their bar codes. Quality filters removed sequences with lengths of less than 300 bases and those with more than two changes in the forward primer portion. PCR chimeras were filtered out using DECIPHER (Wright et al. 2012). The 16S rRNA gene surveys produced a total of 33,733 effective reads for the 12 AS samples, including the triplicates of one control and three exposure treatments, and each sample was covered by 1968–5516 sequences. For analyses, samples were subsampled to 1968 sequences per sample. The raw reads have been deposited into the NCBI short-reads archive database (Accession number: PRJEB4623).

2.4. Data analysis

Sequences were aligned using the secondary structure-based alignment tool INFERNAL (version 0.81) and bacteria 16S rRNA secondary–structure model (Cannone et al. 2002). Operational taxonomic units (OTUs) were defined at 3% distance using RDP's complete linkage clustering tool. Representative sequences for each OTU were classified using RDP's classifier with a 50% bootstrap confidence (Claesson et al. 2009; Wang et al. 2007). On the basis of these clusters, rarefaction curves, Shannon index, Simpson index, Chao1 richness, abundance coverage-based estimator (ACE) and species evenness were calculated using R environment (version 2.15.2; http://www.R-project.org.) with the packages vegan (Oksanen et al. 2013) and phyloseq (McMurdie and Holmes, 2013). Significant change for microbial abundance is considered when p value is less than 0.05. Based on abundance, top ten sensitive (the highest average abundance decrease) or resistant (the highest average abundance increase) genera were listed and depicted in a heat map constructed by R environment (version 2.15.2; http://www.R-project.org.).

2.5. Quantification of gene amoA by qPCR

Degenerate primers, *amoA*-1F (GGGGTTTCTACTGGTGGT) and *amoA*-2R (CCCCTCKGSAAAGCCTTCTTC), targeting ammonia monooxygenase subunit A (*amoA*), were used to quantify its copy number in AS samples. Quantitative PCR was performed using a 7500 real time PCR system from Applied Biosystems (Carlsbad, CA) in 15 μl of reaction mixture composed of 10 ng DNA, SYBR Green Master Mix (7.5 μl), 0.3 μM of each primer and water. Genomic DNA of *Nitrosomonas europaea*, extracted with the same extraction kit for pyrosequencing, was used as the standard.

2.6. Microscopic characteristics of AS

The AS samples were centrifuged (5000 r.p.m., 5 min at 4 °C) and washed with 0.1 M phosphate buffer solution (PBS, pH 7.4). The sludge samples were fixed in 0.1 M PBS with 4% glutaraldehyde overnight at 4 °C, and then sliced in half after freezing in liquid nitrogen (Fang and Chui, 1993). The samples were dehydrated in a series of water/ethanol solutions (20, 40, 60, 80, 100%, vol/vol) for 10–15 min (Jeon et al. 2000), then treated with a mixture of ethanol and *tert*-butanol (1:1) for 10 min, and placed on a stub. The AS microstructure was examined using a FEI Quanta 400 environmental scanning electron microscopy (FEI Co., Hillsboro, Oregon), after the samples were sputter-coated with gold under vacuum. Duplicates were performed for each control and silver treatment, and at least 10 different locations on a grid were observed.

3. Results and discussion

3.1. AgNPs affect the AS community structure to a greater extent than Ag^+

The impact on microbial community structure increased from exposure to Ag^+ (added as $AgNO_3$) to 5-nm AgNPs to 35-nm AgNPs (Fig. 1), with the latter treatment also experiencing a significant decrease in microbial diversity, although one of the control replicates was an outlier. Notably, the total silver concentration of 5-nm AgNPs was 20-fold lower than that used in the Ag^+ treatments, but had a greater effect on the microbial community. This is surprising because AgNPs were recently demonstrated to exert no antimicrobial activity in the absence of Ag^+ release, implying that Ag^+ is the critical effector of the antibacterial activity of AgNPs (Xiu et al. 2012).

High concentrations of Cl^-, SO_4^{2-} and CO_3^{2-} were present in the AS samples (Table S2), and these ions could chelate Ag^+ and decrease its bioavailability and impact. To assess the prevailing dissolved silver species in the microcosms, equilibrium speciation modeling was conducted using Visual MINTEQ version 3.0 based on the measured concentrations of the inorganic ligand and dissolved organic matter. Simulations suggest that AgCl and $AgCl_2^-$ were the dominant species for dissolved silver in the microcosms (Table S3), and only about 10% of total Ag salts were available as Ag^+. ICP-MS analysis surprisingly did not detect Ag^+ (<0.001 ppm, Table S3) after exposure to Ag^+ or AgNPs, although the total silver concentrations in each treatment remained constant between

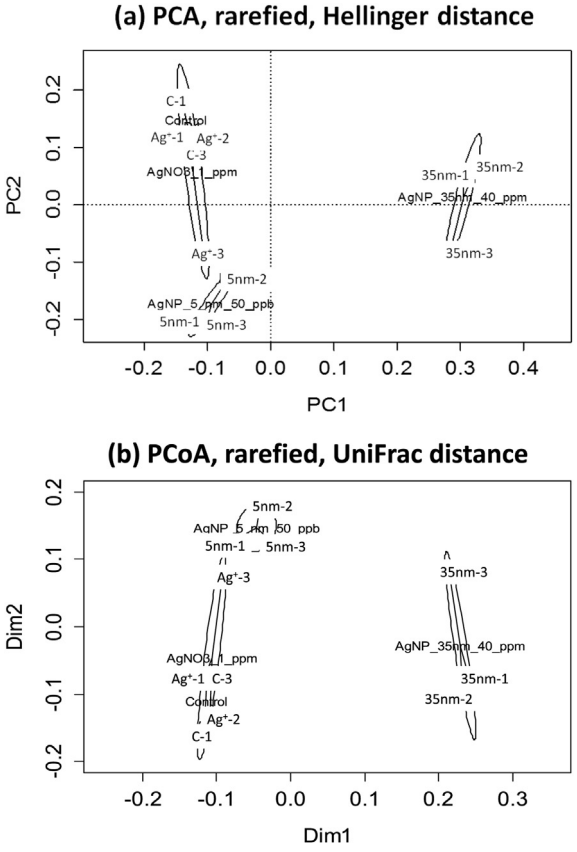

Fig. 1 – Ordination of the microbial communities constructed with principal component analysis (PCA) using Hellinger distance (a) and principal coordinate analysis (PCoA) using UniFrac distance (b). Two control replicates and the Ag^+ triplicates mapped together, indicating a greater similarity among them. All the 5-nm AgNP triplicates mapped a short distance from the control and the 35-nm AgNP triplicates were notably distant.

day 0 and day 7 (Table S4). This suggests that organic matter and inorganic ligands in AS associated with Ag^+, reducing its bioavailability and toxicity, while AgNPs are less susceptible to such scavenging and may more effectively reach bacteria (Morones et al. 2005; Xiu et al. 2011).

Compared to controls and Ag^+-treated samples, exposure to AgNPs elicited changes in the microbial community that could hinder AS performance (Fig. 2). Pyrosequencing showed that all treated and control microbial communities were dominated by *Proteobacteria*, which accounted for 32.9–45.7% of total bacterial sequences. Within *Proteobacteria*, α- and γ-*Proteobacteria* became more abundant ($p < 0.05$) upon exposure to 35-nm AgNPs (Fig. S2); in contrast, β- and δ-*Proteobacteria* were less abundant after exposure to 5-nm and 35-nm AgNPs, respectively. Since *Proteobacteria* are important for AS process performance (Jeon et al. 2003), such as organic waste, phosphorus and nitrogen removal, the negative impact of AgNPs on their abundance could adversely influence the performance of WWTPs.

Other abundant phyla found in the AS samples included *Acidobacteria* (7.7–17.9%), *Chloroflexi* (4.8–13.5%), *Gemmatimonadetes* (2.1–3.4%), *Bacteroidetes* (0.7–4.4%), *Firmicutes* (1.0–1.8%) and *Actinobacteria* (0.6–1.0%), consistent with previous studies of AS communities (Zhang et al. 2012). *Chlamydiae*, which was present in all control replicates, was absent in all three silver treatments, demonstrating their high sensitivity to AgNPs and Ag^+, likely due to the absence of heavy metal efflux systems (which endow metal resistance) (Nies, 2003). In the 5-nm AgNP treatments, *Chlorobi* was less abundant, but the abundance of WS3 was increased significantly, along with *Gemmatimonadetes* and *Bacteroidetes*. The tolerance of *Sphingobacteria* (Fig. S3), which is associated with rapid degradation of labile organics (Acosta-Martinez et al. 2008), accounted for most of the increased abundance of *Bacteroidetes*. The *Bacteroidetes* are known to promote sludge foaming and bulking (Kragelund et al. 2008), both of which interfere with AS performance and increase WWTP operating costs.

Table 1 – Quantification of ammonia monooxygenase subunit A gene (*amoA*) in control and silver treatments. Significant reduction of its copy number was observed in the AS sample exposed to 35-nm AgNPs, suggesting potential adverse effect of 35-nm AgNPs on nitrification.

Treatment	Copy number ($\times 10^7$) of gene *amoA* in 1 ng AS genomic DNA
Control	21.0 ± 2.8
$AgNO_3$	30.0 ± 3.8
5-nm AgNPs	26.2 ± 1.6
35-nm AgNPs	4.0 ± 1.3

The impact on microbial community structure was much more pronounced following exposure to 35-nm AgNPs, which decreased the abundance of *Chloroflexi*, *Firmicutes* and *WS3*, but increased the population of *Acidobacteria*. In *Chloroflexi*, *Anaerolineae* were significantly less abundant (Fig. S4); for *Acidobacteria*, 35-nm AgNPs significantly increased the abundance of class *Gp4* and *Gp17*, as well as that of *Gp22* and *Holophaga* (Fig. S5).

3.2. Decrease in abundance of nitrifying bacteria

Biological nitrogen removal is an important AS process, and nitrification is often the rate-limiting step (Wagner et al. 2002). Nitrifying bacteria are classified as either ammonia- or nitrite-oxidizing. Previously we reported the vulnerability of the ammonia-oxidizer *N. europaea* to 35-nm AgNPs (Yang et al. 2013). Here, we observed a significant decrease in abundance of *Nitrosomonas*, and the absence of *Nitrosococcus*, in the 35-nm AgNP treatments. AgNPs also reduced the abundance of

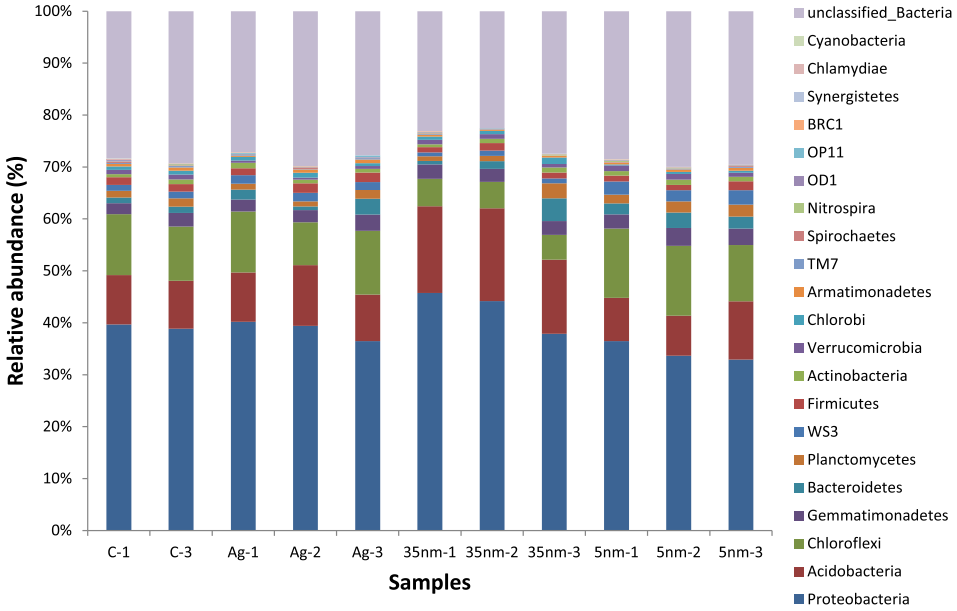

Fig. 2 – Relative abundance of phyla in Ag-exposed AS samples and the controls. The abundance for each phylum, classified by RDP Classifier at a confidence threshold of 50%, is displayed as percentage of total bacterial sequences in each sample.

Chloroflexi that can participate in carbon oxidation and nitrification (Kragelund et al. 2007). A four-fold decrease in copy number of the ammonia monooxygenase subunit A gene (*amoA*), used as a functional gene marker for ammonia-oxidizing bacteria, was observed in 35-nm AgNP-treated samples using quantitative polymerase chain reaction (qPCR), but not in $AgNO_3$- or 5-nm AgNP-treated samples (Table 1). These results are consistent with the pyrosequencing data, and imply that exposure to 35-nm AgNPs at 40 ppm would have an adverse effect on biological nitrogen removal. Other types of NPs (e.g., ZnO and TiO_2) can also hinder nitrogen removal by AS (Zheng et al. 2011a,b).

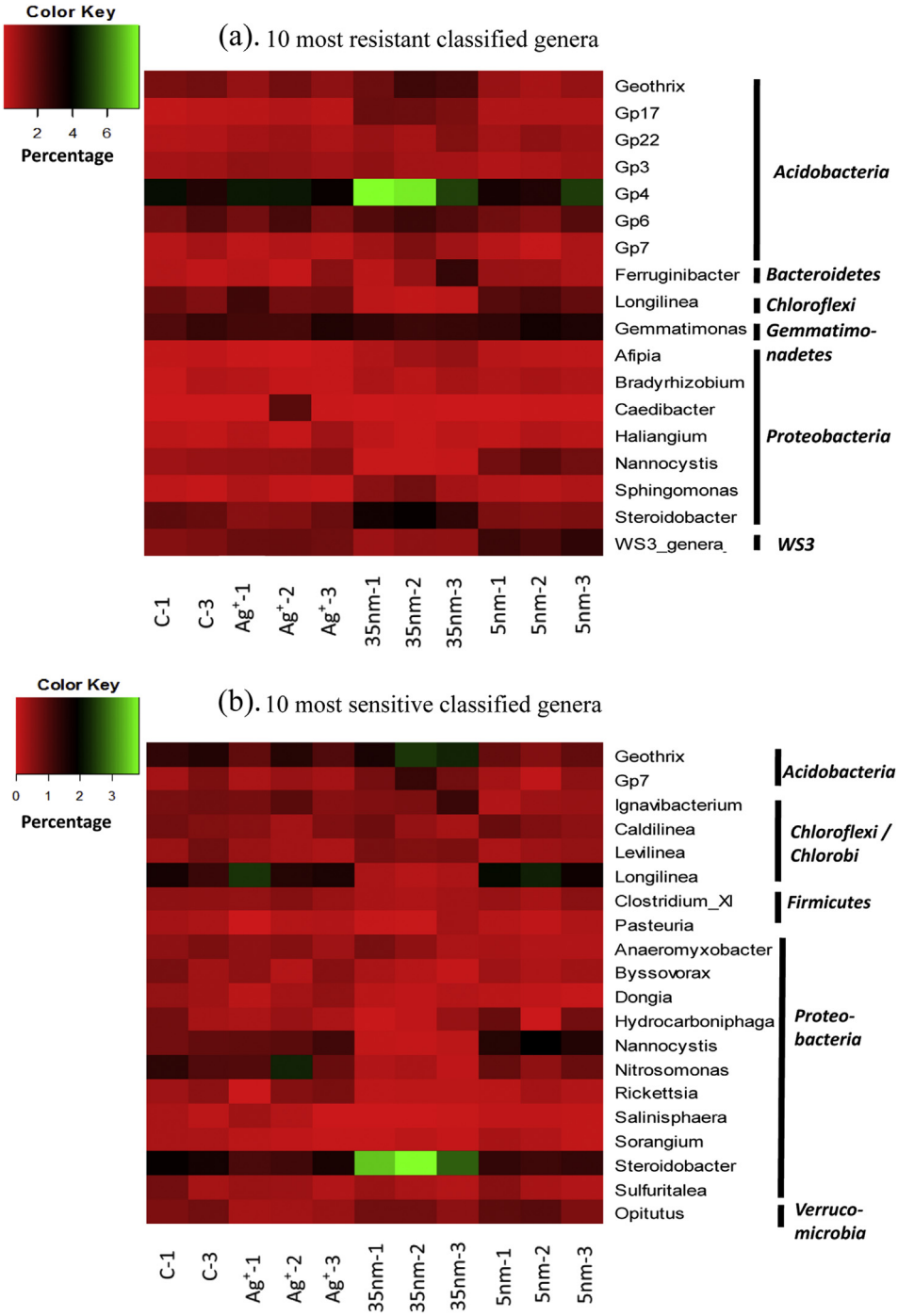

Fig. 3 – Heat-maps of the 10 most resistant classified genera (a) and 10 most sensitive genera (b) in different treatments. The color intensity in each panel represents the relative abundance as the percentage of total bacterial sequences in one sample. *Gp17* and *Steroidobacter* demonstrated great tolerance to AgNPs, and *Longilinea*, *Nannocystis* and *Nitrosomonas* showed high sensitivity to AgNPs. (For interpretation of the references to color in this figure legend, the reader is referred to the web version of this article.)

3.3. *Identification of most sensitive and resistant genera*

A heat-map containing ten genera from each treatment that displayed either the largest increase or decrease in abundance was used to illustrate commonalities in microbial community changes across treatments (Fig. 3). *Acidobacteria* and *Proteobacteria* were the two largest groups (39% and 39% respectively) in the heat-map of silver resistant genera (Fig. 3a). Specifically, *Gp4*, *G22*, and *Ferruginibacter* showed high tolerance to all tested forms of silver. Other resistant genera belonged to phyla *Bacteroidetes*, *Chlorolfexi*, *Gemmatimonadetes* and *WS3*. The ten most sensitive phyla from each silver treatment produced 20 total genera from the phyla *Acidobacteria*, *Chloroflexi/Chlorobi*, *Proteobacteria*, *Verrucomicrobia* and *Firmicutes* (Fig. 3b), with *Proteobacteria* (55%) and *Chloroflexi/Chlorobi* (20%) being the most dominant. For both the resistant

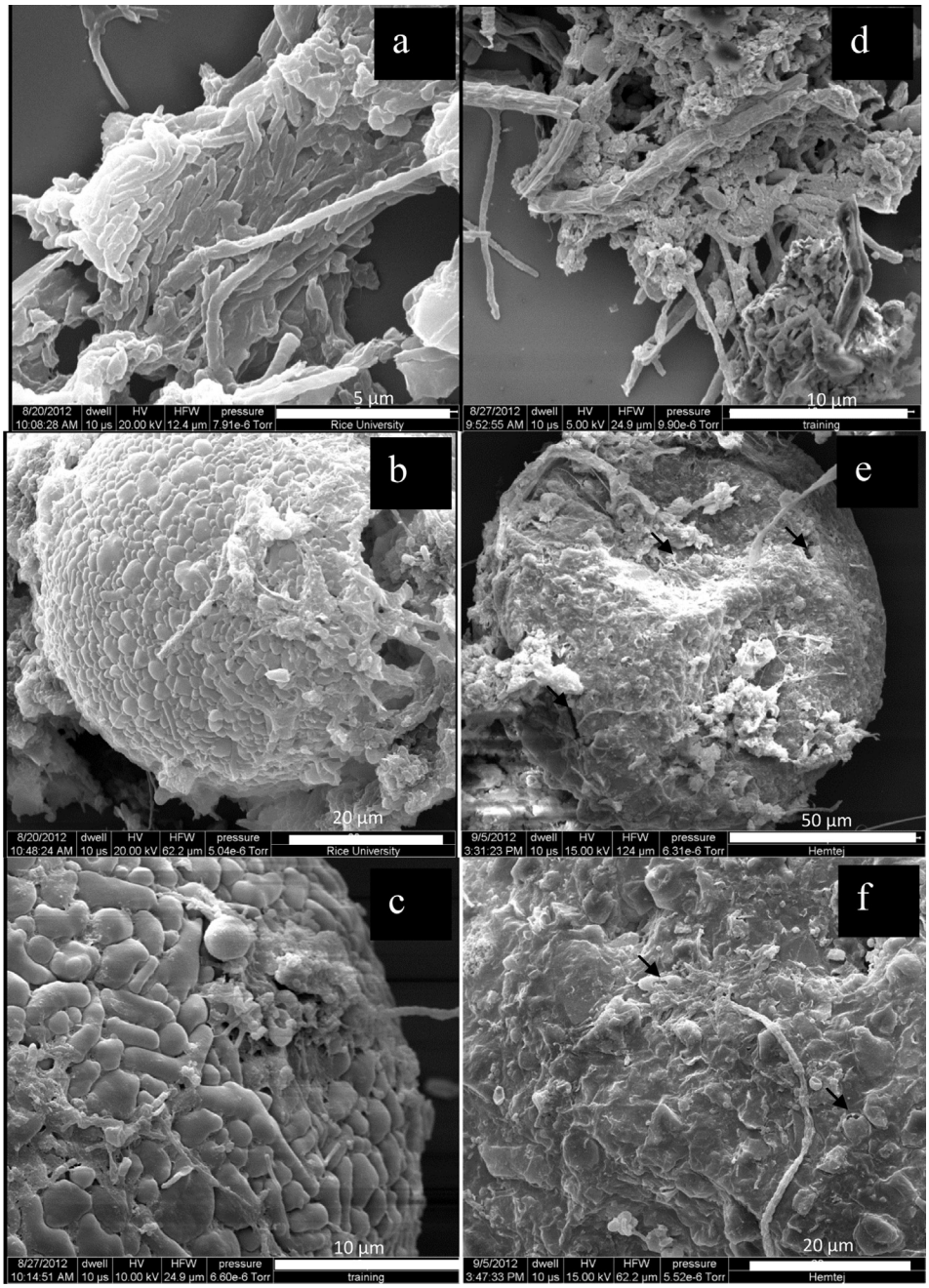

Fig. 4 – SEM images of (a) a typical filamentous interior of granular sludge from the control sample; (b) intact granule from the AgNO3 treatment; (c) packed surface of a granule from the 5-nm AgNP treatment; (d) filamentous interior of granular sludge from a sample exposed to 35-nm AgNPs, (e) granule in 35-nm AgNP samples with a cracked and pitted surface (indicated by black arrows), and (f) surface of the damaged granule (exposed to 35-nm AgNPs) associated with broken cells (indicated by black arrows) and fewer bacteria (compared to panel (c)). More damaged cells were observed after exposure to 35-nm AgNP, and the filamentous interior of granular sludge contained fewer rod-shaped cells.

and sensitive groupings, the 5-nm AgNP treatment shared more genera with both the Ag^+ and 35-nm AgNP treatments than they did with each other (Fig. S6). Surprisingly, some genera such as *Geothrix*, *Gp7*, *Longilinea* and *Nitrosomonas*, were classified as both most sensitive and most resistant depending on the silver treatments (different effect of $AgNO_3$ and 35-nm AgNPs). This observation further supports our hypothesis that the high concentration of 35-nm AgNPs exerted additional pressure on the AS microbial community that was not apparent with $AgNO_3$ exposure. This is likely due to the presence of inorganic ligands and organic chelators in the AS matrix that bind and decrease the bioavailability of Ag^+ to a greater extent than that of AgNPs (Xiu et al. 2011). Accordingly, we postulate that AgNPs that are in close proximity to, or associated with, cell membranes are able to generate higher local Ag^+ concentrations that may lead to higher impact on these genera.

Extrusion of heavy metal ions by efflux systems, segregation by thiol-containing molecules, and reduction into less toxic oxidative states (Nies, 1999) are common bacterial metal resistance mechanisms. Therefore, a prevalence of multiple metal-resistance integrons in certain *γ-Proterobacteria* (Nemergut et al. 2004), secretion of extracellular polymers from some *α-Proterobacteria* (e.g., *Sphingomonas*) (Nilgiriwala et al. 2008), excretion of extracellular slime and siderophores, and possession of genes encoding a variety of ion channels, resistance-nodulation-cell division transporters, and drug transporters in *Acidobacteri* (Ward et al. 2009) can enhance their survival in metal-contaminated environments. On the other hand, a lack of an outer membrane in Gram positive *Pasteuria* and *Clostridium XI*, deficiency of resistance-nodulation-cell division proteins in Gram positive *Clostridium* (Nies, 2003), and absence of a lipid outer membrane and specialized secretion systems (e.g., type I, II and III secretion systems) in *Chloroflexi* (Sutcliffe, 2011) might account for their sensitivity to AgNPs. *Chloroflexi* and *Proteobacteria* play a key role in nutrient removal and AS floc structural stability, which is critical to sludge settling in the secondary clarifier tank and subsequent recycling. Thus, their high sensitivity to AgNPs may negatively affect the performance of AgNP-exposed AS.

3.4. *Damage to AS granules and floc structure*

Scanning electron microscopy (SEM) was used to characterize the effect of AgNPs and Ag^+ on AS floc structure and granulation (Fig. 4). At the concentrations tested, the 35-nm AgNPs damaged AS granules, whereas no difference in floc structure was observed between the control and samples exposed to Ag^+ or 5-nm AgNPs. In control, Ag^+ or 5-nm AgNP treatments, sludge granules (40–70 μm) with compact outer structures were observed (Fig. 4b and c) and, inside the granules, most of rod-shaped bacteria were clustered, associating with filamentous microbes (Fig. 4a). In 35-nm AgNP treatments, we observed more damaged cells and granules with cracked and pitted surfaces (Fig. 4d,e and f), as well as less filamentous cells, probably due to the higher exposure concentrations used for 35-nm AgNPs. Filamentous bacteria such as *Chloroflexi* are important structural components of AS flocs, and AS exposure to 35-nm AgNPs decreased their abundance, as well as that of other filamentous bacteria (e.g., certain *Proteobacteria*, *Actinobacteria* and *Firmicutes*). Overall, these observations suggest that AgNPs damage AS granules and floc structure, which would hinder setting processes that are critical to AS operation (i.e., clarification and sludge recycle).

4. Conclusions

Compared to unamended controls and Ag^+ treatment, AS exposure to AgNPs resulted in more pronounced changes in community structure, such as a significant reduction in species richness and over 50% decrease in *Chloroflexi* abundance. Differential susceptibilities to AgNPs promoted a shift in microbial community structure towards more silver-tolerant species (e.g., *Acidobacteria* and *Bacteroidetes*). Since nitrifying bacteria (e.g., *Nitrosomonas* and *Nitrosococcus*) and *Chloroflexi* involved in nitrification were differentially impacted by AgNPs, this finding underscores a potential threat to nitrogen removal. AgNPs could also damage AS granules and floc structure, which could hinder sludge settling and recycling operations. Since WWTPs serve as sinks for urban and industrial releases that could contain AgNPs, further studies are needed to monitor silver fluxes and explore barrier alternatives that protect against inhibitory effects and possible temporary system failure.

Acknowledgments

The authors thank Vicki Colvin, Qingbo Zhang and Hema Puppala for providing 5-nm AgNPs. This research was supported by a Joint U.S.-U.K. research program (U.S.-EPA and U.K-NERC-ESPRC) (EPA-G2008-STAR-R1).

Appendix A. Supplementary data

Supplementary data related to this article can be found at http://dx.doi.org/10.1016/j.watres.2013.09.046.

REFERENCES

Acosta-Martinez, V., Dowd, S., Sun, Y., Allen, V., 2008. Tag-encoded pyrosequencing analysis of bacterial diversity in a single soil type as affected by management and land use. Soil Biol. Biochem. 40 (11), 2762–2770.

Arnaout, C.L., Gunsch, C.K., 2012. Impacts of silver nanoparticle coating on the nitrification potential of *Nitrosomonas europaea*. Environ. Sci. Technol. 46 (10), 5387–5395.

Cannone, J.J., Subramanian, S., Schnare, M.N., Collett, J.R., D'Souza, L.M., Du, Y.S., Feng, B., Lin, N., Madabusi, L.V., Muller, K.M., Pande, N., Shang, Z.D., Yu, N., Gutell, R.R., 2002. The Comparative RNA Web (CRW) Site: an online database of comparative sequence and structure information for ribosomal, intron, and other RNAs. Bmc Bioinforma. 3.

Choi, O.K., Hu, Z.Q., 2009. Nitrification inhibition by silver nanoparticles. Water Sci. Technol. 59 (9), 1699–1702.

Claesson, M.J., O'Sullivan, O., Wang, Q., Nikkila, J., Marchesi, J.R., Smidt, H., de Vos, W.M., Ross, R.P., O'Toole, P.W., 2009.

Comparative analysis of pyrosequencing and a phylogenetic microarray for exploring microbial community structures in the human distal intestine. PLoS One 4 (8).
Cole, J.R., Wang, Q., Cardenas, E., Fish, J., Chai, B., Farris, R.J., Kulam-Syed-Mohideen, A.S., McGarrell, D.M., Marsh, T., Garrity, G.M., Tiedje, J.M., 2009. The Ribosomal Database Project: improved alignments and new tools for rRNA analysis. Nucleic Acids Res. 37, D141–D145.
Fang, H.H.P., Chui, H.K., 1993. Microstructural analysis of anaerobic granules. Biotechnol. Tech. 7 (7), 407–410.
Ge, Y., Schimel, J.P., Holden, P.A., 2012. Identification of soil bacteria susceptible to TiO_2 and ZnO nanoparticles. Appl. Environ. Microbiol. 78 (18), 6749–6758.
Gottschalk, F., Sonderer, T., Scholz, R.W., Nowack, B., 2009. Modeled environmental concentrations of engineered nanomaterials (TiO_2, ZnO, Ag, CNT, fullerenes) for different regions. Environ. Sci. Technol. 43 (24), 9216–9222.
Ip, M., Lui, S.L., Poon, V.K.M., Lung, I., Burd, A., 2006. Antimicrobial activities of silver dressings: an *in vitro* comparison. J. Med. Microbiol. 55 (1), 59–63.
Jeon, C.O., Lee, D.S., Park, J.M., 2000. Morphological characteristics of microbial sludge performing enhanced biological phosphorus removal in a sequencing batch reactor fed with glucose as sole carbon source. Water Sci. Technol. 41 (12), 79–84.
Jeon, C.O., Lee, D.S., Park, J.M., 2003. Microbial communities in activated sludge performing enhanced biological phosphorus removal in a sequencing batch reactor. Water Res. 37 (9), 2195–2205.
Kaegi, R., Voegelin, A., Sinnet, B., Zuleeg, S., Hagendorfer, H., Burkhardt, M., Siegrist, H., 2011. Behavior of metallic silver nanoparticles in a pilot wastewater treatment plant. Environ. Sci. Technol. 45 (9), 3902–3908.
Kim, B., Park, C.S., Murayama, M., Hochella, M.F., 2010. Discovery and characterization of silver sulfide nanoparticles in final sewage sludge products. Environ. Sci. Technol. 44 (19), 7509–7514.
Klasen, H.J., 2000. A historical review of the use of silver in the treatment of burns. II. Renewed interest for silver. Burns 26 (2), 131–138.
Kragelund, C., Levantesi, C., Borger, A., Thelen, K., Eikelboom, D., Tandoi, V., Kong, Y., Krooneman, J., Larsen, P., Thomsen, T.R., Nielsen, P.H., 2008. Identity, abundance and ecophysiology of filamentous bacteria belonging to the Bacteroidetes present in activated sludge plants. Microbiology 154, 886–894.
Kragelund, C., Levantesi, C., Borger, A., Thelen, K., Eikelboom, D., Tandoi, V., Kong, Y.H., van der Waarde, J., Krooneman, J., Rossetti, S., Thomsen, T.R., Nielsen, P.H., 2007. Identity, abundance and ecophysiology of filamentous Chloroflexi species present in activated sludge treatment plants. FEMS Microbiol. Ecol. 59 (3), 671–682.
Liang, Z.H., Das, A., Hu, Z.Q., 2010. Bacterial response to a shock load of nanosilver in an activated sludge treatment system. Water Res. 44 (18), 5432–5438.
Liu, J., Sonshine, D.A., Shervani, S., Hurt, R.H., 2010. Controlled release of biologically active silver from nanosilver surfaces. Acs Nano 4 (11), 6903–6913.
McMurdie, P.J., Holmes, S., 2013. phyloseq: an r package for reproducible interactive analysis and graphics of microbiome census data. PLoS One 8 (4), e61217.
Morones, J.R., Elechiguerra, J.L., Camacho, A., Holt, K., Kouri, J.B., Ramirez, J.T., Yacaman, M.J., 2005. The bactericidal effect of silver nanoparticles. Nanotechnology 16 (10), 2346–2353.
Nemergut, D.R., Martin, A.P., Schmidt, S.K., 2004. Integron diversity in heavy-metal-contaminated mine tailings and inferences about integron evolution. Appl. Environ. Microbiol. 70 (2), 1160–1168.
Nies, D.H., 1999. Microbial heavy-metal resistance. Appl. Microbiol. Biotechnol. 51 (6), 730–750.
Nies, D.H., 2003. Efflux-mediated heavy metal resistance in prokaryotes. FEMS Microbiol. Rev. 27 (2–3), 313–339.
Nilgiriwala, K.S., Alahari, A., Rao, A.S., Apte, S.K., 2008. Cloning and overexpression of alkaline phosphatase PhoK from Sphingomonas sp strain BSAR-1 for bioprecipitation of uranium from alkaline solutions. Appl. Environ. Microbiol. 74 (17), 5516–5523.
Oksanen, J., Blanchet, F.G., Kindt, R., Legendre, P., Minchin, P.R., O'Hara, R.B., Simpson, G.L., Solymos, P., Stevens, M.H.H., Wagner, H., 2013. Vegan: Community Ecology Package. http://vegan.r-forge.r-project.org/.
Qian, P.Y., Wang, Y., Lee, O.O., Lau, S.C.K., Yang, J.K., Lafi, F.F., Al-Suwailem, A., Wong, T.Y.H., 2011. Vertical stratification of microbial communities in the Red Sea revealed by 16S rDNA pyrosequencing. ISME J. 5 (3), 507–518.
Radniecki, T.S., Stankus, D.P., Neigh, A., Nason, J.A., Semprini, L., 2011. Influence of liberated silver from silver nanoparticles on nitrification inhibition of *Nitrosomonas europaea*. Chemosphere 85 (1), 43–49.
Shafer, M.M., Overdier, J.T., Armstong, D.E., 1998. Removal, partitioning, and fate of silver and other metals in wastewater treatment plants and effluent-receiving streams. Environ. Toxicol. Chem. 17 (4), 630–641.
Simpson, S., 2003. Bacterial silver resistance: molecular biology and uses and misuses of silver compounds. FEMS Microbiol. Rev. 27 (2–3), 341–353.
Sutcliffe, I.C., 2011. Cell envelope architecture in the Chloroflexi: a shifting frontline in a phylogenetic turf war (vol. 13, pg 279, 2011). Environ. Microbiol. 13 (8), 2387.
The Project on Emerging Nanotechnologies http://www.nanotechproject.org/.
Wagner, M., Loy, A., Nogueira, R., Purkhold, U., Lee, N., Daims, H., 2002. Microbial community composition and function in wastewater treatment plants. Antonie Van Leeuwenhoek Int. J. General Mol. Microbiol. 81 (1–4), 665–680.
Wang, Q., Garrity, G.M., Tiedje, J.M., Cole, J.R., 2007. Naive Bayesian classifier for rapid assignment of rRNA sequences into the new bacterial taxonomy. Appl. Environ. Microbiol. 73 (16), 5261–5267.
Ward, N.L., Challacombe, J.F., Janssen, P.H., Henrissat, B., Coutinho, P.M., Wu, M., Xie, G., Haft, D.H., Sait, M., Badger, J., Barabote, R.D., Bradley, B., Brettin, T.S., Brinkac, L.M., Bruce, D., Creasy, T., Daugherty, S.C., Davidsen, T.M., Deboy, R.T., Detter, J.C., Dodson, R.J., Durkin, A.S., Ganapathy, A., Gwinn-Giglio, M., Han, C.S., Khouri, H., Kiss, H., Kothari, S.P., Madupu, R., Nelson, K.E., Nelson, W.C., Paulsen, I., Penn, K., Ren, Q.H., Rosovitz, M.J., Selengut, J.D., Shrivastava, S., Sullivan, S.A., Tapia, R., Thompson, L.S., Watkins, K.L., Yang, Q., Yu, C.H., Zafar, N., Zhou, L.W., Kuske, C.R., 2009. Three genomes from the phylum *Acidobacteria* provide insight into the lifestyles of these microorganisms in soils. Appl. Environ. Microbiol. 75 (7), 2046–2056.
Wright, E.S., Yilmaz, L.S., Noguera, D.R., 2012. DECIPHER, a search-based approach to chimera identification for 16S rRNA sequences. Appl. Environ. Microbiol. 78 (3), 717–725.
Xiu, Z.M., Ma, J., Alvarez, P.J.J., 2011. Differential effect of common ligands and molecular oxygen on antimicrobial activity of silver nanoparticles *versus* silver ions. Environ. Sci. Technol. 45 (20), 9003–9008.
Xiu, Z.M., Zhang, Q.B., Puppala, H.L., Colvin, V.L., Alvarez, P.J., 2012. Negligible particle-specific antibacterial activity of silver nanoparticles. Nano Lett. 12 (8), 4271–4275.
Yang, Y., Wang, J., Xiu, Z., Alvarez, P.J., 2013. Impacts of silver nanoparticles on cellular and transcriptional activity of nitrogen cycling bacteria. Environ. Toxicol. Chem. 32 (7), 1488–1496.

Yang, Y., Wang, J., Zhu, H.G., Colvin, V.L., Alvarez, P.J., 2012. Relative susceptibility and transcriptional response of nitrogen cycling bacteria to quantum dots. Environ. Sci. Technol. 46 (6), 3433–3441.

Yang, Y., Zhu, H.G., Colvin, V.L., Alvarez, P.J., 2011. Cellular and transcriptional response of *Pseudomonas stutzeri* to quantum dots under aerobic and denitrifying conditions. Environ. Sci. Technol. 45 (11), 4988–4994.

Zhang, T., Shao, M.F., Ye, L., 2012. 454 Pyrosequencing reveals bacterial diversity of activated sludge from 14 sewage treatment plants. ISME J. 6 (6), 1137–1147.

Zheng, X., Chen, Y.G., Wu, R., 2011a. Long-term effects of titanium dioxide nanoparticles on nitrogen and phosphorus removal from wastewater and bacterial community shift in activated sludge. Environ. Sci. Technol. 45 (17), 7284–7290.

Zheng, X.O., Wu, R., Chen, Y.G., 2011b. Effects of ZnO nanoparticles on wastewater biological nitrogen and phosphorus removal. Environ. Sci. Technol. 45 (7), 2826–2832.